JOURNAL OF SOLID STATE CHEMISTRY 33, 341–350 (1980)

$Ba_3WFe_2O_9$ ($P6_3/mmc$) and $Ba_3WFe_2O_{8.42(5)}$ ($Fm3m$): Comparative Study of the Crystallographical and Magnetic Properties

G. MATZEN AND P. POIX

Département Science des Matériaux, ERA 679, ENSCS, 1, rue Blaise Pascal, B.P. 296/R8, 67008 Strasbourg Cedex, France

Received July 16, 1979; in revised form October 15, 1979

$Ba_3WFe_2O_9$ has a hexagonal structure which belongs to space group $P6_3/mmc$. Heated at 1350°C under a stream of helium, this compound gives an oxygen-deficient phase, the structure of which is ordered cubic (space group $Fm3m$). This passage from a hexagonal structure to a cubic structure is consistent with the decrease of the Goldschmidt tolerance factor resulting from the Fe^{3+} partial reduction. $Ba_3WFe_2O_{8.42(5)}$ (cubic) was compared with $Ba_3WFe_2O_9$ (hexagonal) and $Sr_3WFe_2O_{8.85(3)}$ (cubic) as to the crystallographical and magnetic properties. The study of the thermal stability in air for $Ba_3WFe_2O_{8.42(5)}$ revealed a reoxidation in several steps and the existence of a new cubic compound, stable in air over a broad range of temperature, the formula of which may be written as $Ba_3WFe_2O_{8.71(5)}$.

Introduction

The preparation in air of $Ba_3WFe_2O_9$ (*1*) leads to a slightly overoxidized phase. So we tried to prepare this compound in an evacuated silica ampoule, then under a stream of helium. This second procedure gave products which showed significant weight changes while the corresponding X-ray photographs indicated two phases (*2*). A careful study of this phenomenon led to a partially reduced phase with a cubic structure, which we studied and compared with similar compounds.

Preparation

$Ba_3WFe_2O_9$ was first prepared from a stoichiometric mixture of oxides and carbonate by firing in air, according to the equation:

$$3\ BaCO_3 + WO_3 + Fe_2O_3 \rightarrow Ba_3WFe_2O_9 + 3\ CO_2\uparrow.$$

The stoichiometric mixtures of the starting materials were hand mixed in an agate mortar and heated in Pt crucibles at 1300°C in air for 6 hr. X-Ray examination revealed a hexagonal phase which belongs to space group $P6_3/mmc$ (*1*). But the products were shown by their X-ray photographs to contain always small amounts of $BaWO_4$ (Photograph 1a) in addition to the hexagonal phase (Photograph 1b). The presence of $BaWO_4$ can be explained by the following equilibrium:

$$Ba_3WFe_2O_9 + x(\tfrac{1}{2} - \alpha)O_2 \rightleftarrows (1 - x)Ba_3WFe_2O_9 + x(BaWO_4 + 2\ BaFeO_{3-\alpha}).$$

$BaFeO_{3-\alpha}$ (*3*) which has the same structure as $Ba_3WFe_2O_9$ forms a solid solution with this compound, and so does not appear on the X-ray patterns, unlike $BaWO_4$, which does appear. We studied this overoxidation mechanism in detail in the case of $Sr_3WFe_2O_9$ which contains also a small

0022-4596/80/090341-10$02.00/0

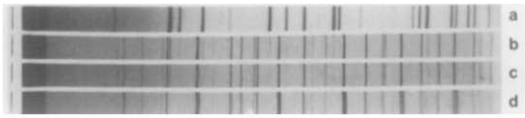

PHOTOGRAPH 1. Powder X-ray diffraction photograph of (a) $BaWO_4$, (b) $Ba_3WFe_2O_9$ (air), (c) $Ba_3WFe_2O_9$ (silica ampoule), and (d) $Ba_3WFe_2O_{9-x}$ (He).

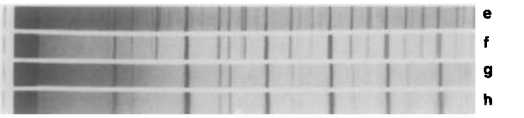

PHOTOGRAPH 2. Powder X-ray diffraction photograph of (e) $Ba_3WFe_2O_9$ (air), (f) $Ba_3WFe_2O_{9-x}$ (He), (g) $Ba_3WFe_2O_{8.4}$ (He), and (h) $Ba_3WFe_2O_{8.4+x}$ (a reoxidation product of $Ba_3WFe_2O_{8.4}$).

quantity of $SrWO_4$ when it is prepared in air (*4*).

The preparation of $Ba_3WFe_2O_9$ from Ba_3WO_6 and Fe_2O_3 in an evacuated silica ampoule gave a product which was a bit more pure as shown by X-ray examination. The reflections of $BaWO_4$ are a little weaker (Photograph 1c), but always present. Therefore, we tried to prepare $Ba_3WFe_2O_9$ under a stream of inert gas.

The product prepared in air was heated at 1350°C under a flow of helium. The compound first lost some oxygen but remained hexagonal while the lattice constants slightly changed. Then, a mixture of two phases appeared, a hexagonal phase and a cubic phase (Photograph 1d). The intensity of the cubic structure reflections increased progressively, whereas the hexagonal phase reflections became weaker and weaker and finally disappeared after a few hours of firing. The smallest substoichiometry that leads to a pure cubic phase corresponds to the formula $Ba_3WFe_2O_{8.5(1)}$.

We also tried to get the cubic phase from stoichiometric mixtures of the following type:

$$Ba_3WO_6 + (1 - y)Fe_2O_3 + 2yFe.$$

This procedure using also a stream of helium directly gave a cubic phase of which the formula can be written as $Ba_3WFe_2O_{9-x}$. The nonstoichiometry of this phase varies in the range $0.5 < x < 0.8$. It depends on the quantity of metal iron present in the starting mixture and also on the temperature and time of heating. If the substoichiometry is extensive ($x > 0.6$), the corresponding compounds are not very stable. Therefore, we essentially studied $Ba_3WFe_2O_{8.42(5)}$ (Photograph 2g), a pure cubic compound directly prepared from Ba_3WO_6, at the limit of the two-phase domain, and stable in air at room temperature.

Stability in Air

The thermal stability in air of $Ba_3WFe_2O_{8.4}$ was investigated by a thermobalance study. The variation curve of weight as a function of temperature revealed a reoxidation in several steps (Table I). The observed reactions paths which correspond to the reduction at a high temperature on the one hand and to the reoxidation at a moderately high temperature on the other hand are not the same although the products are identical at the beginning and at the end of the reactions.

This phenomenon may be explained in the following way. For the reduction at 1350°C under a stream of helium, the temperature is high enough to permit the hexagonal cell to cross the energy barrier which separates it from the cubic cell, more stable when the Fe^{2+} percentage becomes important. At the beginning of the reoxidation, on the contrary, the temperature is too low to permit the Fe^{2+} cations to reoxidize rapidly and the cubic cell to cross the energy barrier and transform to the hexagonal cell. Therefore, the compound slowly reoxidizes and gives $Ba_3WFe_2O_{8.71(5)}$, a new cubic compound. This limit composition seems to correspond to the highest Fe^{3+} percentage the cubic structure can contain

TABLE I

THERMOGRAVIMETRIC STUDY OF $Ba_3WFe_2O_{8.42(5)}$: REOXIDATION STEPS

Temperature range (°C)	Observed weight	Corresponding product
$T < 100$	Constant	$Ba_3WFe_2O_{8.42(5)}$
$100 < T < 500$	Increasing	$Ba_3WFe_2O_{8.42+x}$
$500 < T < 750$	Constant	$Ba_3WFe_2O_{8.71(5)}$
$750 < T < 1200$	Increasing	$Ba_3WFe_2O_{8.71+x}$
$1200 < T$	Constant	$Ba_3WFe_2O_9 + \epsilon\ BaWO_4$

without being distorted. A further reoxidation needs a higher temperature and is responsible for a cubic cell distortion (Photograph 2h) before the passage to the hexagonal structure.

Structure Determination

Structural Change and Factor t

It appears experimentally that the perovskite-related phases of the general formula ABO_3 have a structure which depends on the tolerance factor t introduced by Goldschmidt and defined as:

$$t = (r_A + r_O)/2^{1/2}(r_B + r_O),$$

where r_A, r_B, and r_O are the respective ionic radii of the A and B cations and the O^{2-} anion. A more precise value of this tolerance factor can be obtained if the ionic radii are replaced by the characteristic anion–cation distances introduced by Poix (*5*). Then the expression of t is the following:

$$t = \theta/(2^{1/2} \times \beta),$$

where β and θ are, respectively, the anion–cation distances for 6-coordinate and 12-coordinate cations.

For the $A_3B_2B'O_9$ oxides, $t = 1$ is the limit between the cubic domain ($t \leq 1$) and the hexagonal domain ($t > 1$). The few compounds listed in Table II illustrate the variation of factor t as a function of the cations present in the structure (*6*).

The factor t may be calculated in the case of the studied compound $Ba_3WFe_2O_{8.5(1)}$:

$\beta(Fe^{2+}) = 2.147$ Å, $\beta(Fe^{3+}) = 2.020$ Å, $\beta(W^{6+}) = 1.900$ Å, $\theta(Ba^{2+}) = 2.886$ Å,

$\bar{\beta} = \frac{1}{3}[1.900 + 2.020(1 + \epsilon \times 0.2) + 2.147(1 - \epsilon \times 0.2)]$,
$= 2.022(9)$ Å $\quad (\epsilon = \pm 1)$,
$t = 2.886/(2^{1/2} \times 2.022)$,
$= 1.009(5)$.

Indeed, the passage from the hexagonal structure to the cubic structure corresponds to a decrease of t which is equal to 1.031 for $Ba_3WFe_2O_9$ and to 1.009(5) for $Ba_3WFe_2O_{8.5(1)}$.

Hexagonal and Cubic Structures

The space groups of the hexagonal and cubic structures are, respectively, $P6_3/mmc$ ($6H$) and $Fm3m$, the symmetries of which are quite different. But in fact, both structures can be described as close-packed BaO_3 layers (*7*). Fe^{n+} ($n = 2$ or 3) and W^{6+} occupy octahedral sites: $2a$ and $4f$ in the hexagonal structure (*8*), $4a$ and $4b$ in the cubic structure (*9*). Because of the structural characteristics common to these two stackings, the X-ray photographs of $Ba_3WFe_2O_9$ and $Ba_3WFe_2O_{8.4}$ show the same intense reflections characteristic of

the ABO_3 perovskite (Photographs 2e and g).

The close-packed AO_3 layers are the (001) planes perpendicular to the c axis in the hexagonal lattice and the (111) planes perpendicular to the [111] direction in the cubic lattice. In addition the experimental values of the lattice parameters are:

$Ba_3WFe_2O_9$ (*1*): $a = 5.770(2)$ Å,
$c = 14.140(15)$ Å,

$Ba_3WFe_2O_{8.42(5)}$: $a' = 8.105(2)$ Å.

The comparison of a and c with a' gives the following relations:

$$a'\,2^{1/2}/2 = 5.701 \text{ Å} \lesssim 5.770 \text{ Å } (=a),$$
$$a'\,3^{1/2} = 13.964 \text{ Å} \lesssim 14.140 \text{ Å } (=c).$$

Consequently, one may construct the ideal hexagonal cell corresponding to the cubic cell by a simple axis change:

$$\mathbf{a} = \tfrac{1}{2}(\mathbf{a}' + \mathbf{c}'),$$
$$\mathbf{b} = \tfrac{1}{2}(\mathbf{b}' - \mathbf{c}'),$$
$$\mathbf{c} = -\mathbf{a}' + \mathbf{b}' + \mathbf{c}'.$$

Remarks:

c/a ideal $= a' \times 3^{1/2}/(a' \times 2^{1/2}/2) = 6^{1/2} = 2.4495$,

c/a real $= 14.140/5.770 = 2.4506$,

$(c/a \text{ real} - c/a \text{ ideal})/(c/a) = 0.5‰$.

$$\Delta a/a = 0.3‰, \quad \Delta c/c = 1.1‰, \quad \Delta(c/a)/(c/a) = 1.4‰ > 0.5‰.$$

These results show that no axial distortion can be experimentally observed for the hexagonal cell.

Structural Change and Cell Contraction

Because of this absence of axial distortion, it is possible to associate to the hexagonal cell a cubic cell, the lattice constant of which can be deduced from the parameters of the hexagonal structure:

$$a_1' = a \times 2^{1/2} = 8.160 \text{ Å}$$
$$a_2' = c/3^{1/2} = 8.164 \text{ Å}$$
$$\rightarrow a' \simeq 8.162 \text{ Å } (>8.105 \text{ Å}).$$

When the hexagonal cell transforms to the cubic cell, a volume contraction takes place:

$$\Delta a/a = 0.057/8.162 \simeq 7.0‰ \rightarrow \Delta v/v \simeq 2.1\%.$$

It seems that the passage to the cubic cell leads to a more compact structure. The real hexagonal structures are generally less compact than the corresponding hypothetical cubic structures, the parameters of which can be obtained with the formula calculated by Poix in the case of perovskites (*5*):

$$a = (\beta + \theta)/[(2^{1/2} + 1)/2].$$

For the classical perovskites, the relative error between the measured constant and the calculated constant is about 2‰. For $Sr_3WFe_2O_9$ (cubic), one obtains the following values:

$$a_{meas} = 7.888(2) \text{ Å } (4), \quad a_{calc} = 7.879 \text{ Å} \rightarrow \Delta a/a = 1.1‰.$$

TABLE II

t VALUE AND STRUCTURE FOR A FEW $A_3B_2B'O_9$ COMPOUNDS

Compound	*t*	Structure
$Sr_3WCo_2O_9$	0.978	Cubic
$Sr_3TeFe_2O_9$	0.986	Cubic
$Sr_3WFe_2O_9$	0.991	Cubic
$Ba_3WCo_2O_9$	1.021	Hexagonal
$Ba_3TeFe_2O_9$	1.026	Hexagonal
$Ba_3WFe_2O_9$	1.031	Hexagonal

The parameter corresponding to the hypothetical cubic cell of $Ba_3WFe_2O_9$ is equal to 8.063 Å, however, which is noticeably smaller than the parameter calculated from the real hexagonal structure, 8.162 Å. The cubic cell of $Ba_3WFe_2O_{8.4}$ has a lattice constant of 8.105 Å, i.e., higher than 8.063 Å. But one must take into account the presence of oxygen vacancies and the increase of the average cation size which often lead to a lattice constant increase. For example, $SrFeO_{2.95}$ has a parameter of 3.859(3) Å, whereas it is equal to 3.8695(5) Å for $SrFeO_{2.78}$ (*10*).

Structure Determination of $Ba_3WFe_2O_{8.42(5)}$

The crystallographical data of $Ba_3WFe_2O_{8.4}$ obtained from powder X-ray diffraction patterns were treated with the aid of a FORTRAN program. The cubic lattice constant determined, using NaCl as an internal standard, is equal to 8.105(2) Å. All the lines which appeared on the patterns corresponded to *h*, *k*, and *l* indices with the same parity. In addition, the patterns of $Ba_3WFe_2O_{8.4}$ presented a great analogy with those of $Ba_3UFe_2O_9$ (*11*) (space group $Fm3m$). Therefore we used this group for intensity calculations.

The atom distribution in the cubic cell is summarized in Table III. All the equivalent positions are obtained from those indicated by the translations of the cubic face-centered cell:

$$(0, 0, 0), (\tfrac{1}{2}, 0, 0), (0, \tfrac{1}{2}, 0), (0, 0, \tfrac{1}{2}).$$

The largest cation, Ba^{2+}, occupies a dodecahedral site, whereas W^{6+} and Fe^{n+} are distributed in the 4*a* and 4*b* octahedral sites.

In order to determine the cell completely, one must calculate the values of two variables: x which gives the position of oxygen along the cell edges and λ which reflects the order between W^{6+} and Fe^{n+}. The formula of the cation distribution in the cell depends on the λ value and can be written as:

formula	$Ba_8(Fe_{4-\lambda}W_\lambda)$		$(Fe_{4/3+\lambda}W_{8/3-\lambda})$	$O_{24(1-\epsilon)}$
sites	8*c*	4*a*	4*b*	24*e*

An order rate between the cations in octahedral sites may be deduced from it and defined as:

$$\tau = \frac{(\frac{8}{3} - \lambda) - \lambda}{(\frac{8}{3} - \lambda) + \lambda} \rightarrow \tau = 1 - (\tfrac{3}{4}) \times \lambda.$$

A program was used to get the best values of x and λ. The atomic scattering factors for Ba^{2+}, W^{6+}, Fe^{3+}, and Fe^{2+} were calculated from the tabulation of Cromer and Waber (*12*). Anomalous dispersion corrections were also used (*13*). The oxygen factor was calculated according to the Tokonami function (*14*) for the Cu$K\alpha$ radiation. The best agreement obtained between the calculated and observed intensities (Table IV) corresponds to the following results:

$$x = 0.250(5),$$

$$\tau = 100\%,$$

$$R = 11.5\%.$$

R is defined as $R = \Sigma|I_c - I_o|/\Sigma I_o$, where I_c

TABLE III

ATOM POSITIONS IN THE $Fm\bar{3}m$ UNIT CELL FOR $Ba_3WFe_2O_{8.42(5)}$

Ions	Wyckoff notation	Coordinates of equivalent positions
Ba^{2+}	8*c*	$(\frac{1}{4}, \frac{1}{4}, \frac{1}{4})$ $(\frac{3}{4}, \frac{3}{4}, \frac{3}{4})$ . . .
W^{6+}, Fe^{n+}	4*a*	(0, 0, 0) . . .
W^{6+}, Fe^{n+}	4*b*	$(\frac{1}{2}, \frac{1}{2}, \frac{1}{2})$ . . .
O^{2-}	24*e*	$(x, 0, 0)$ $(0, x, 0)$ $(0, 0, x)$ $(\frac{1}{2} + x, 0, 0)$ $(0, \frac{1}{2} + x, 0)$ $(0, 0, \frac{1}{2} + x)$ . . .

and I_o are, respectively, the calculated and observed intensities.

Comparative Study of $Ba_3WFe_2O_{8.4}$, $Ba_3WFe_2O_9$, and $Sr_3WFe_2O_{8.85}$

It is interesting to compare $Ba_3WFe_2O_{8.4}$ to $Ba_3WFe_2O_{9.0}$ on the one hand and to $Sr_3WFe_2O_{8.85}$ on the other hand. Indeed, this comparison allows one to emphasize the lines of the X-ray patterns which are common to the hexagonal and cubic structures and characteristic of the perovskite ABO_3

TABLE IV

X-RAY POWDER DIFFRACTION DATA FOR $Ba_3WFe_2O_{8.42(5)}$

h k l	I_{obs}	I_{calc}	*h k l*	I_{obs}	I_{calc}
1 1 1	4.9	7.3	8 0 0	3.5	3.7
2 0 0	1.1	1.3	7 3 3	0	0.4
2 2 0	100.0	114.0	6 4 4	0	0.2
3 1 1	5.0	4.7	8 2 0		0.2
2 2 2	6.0	7.7	6 6 0	16.3	5.2
4 0 0	36.7	36.2	8 2 2		10.4
3 3 1	2.2	2.2	5 5 5	1.5	0.1
4 2 0	0.9	0.7	7 5 1		0.8
4 2 2	52.3	46.0	6 6 2	0	1.1
3 3 3	2.8	0.4	8 4 0	14.0	14.6
5 1 1		1.3	7 5 3	1.8	0.8
4 4 0	24.8	21.4	9 1 1		0.4
5 3 1	2.5	1.7	8 4 2	0	0.6
4 4 2	0	0.3	6 6 4	11.2	11.8
6 0 0		0.1	9 3 1	1.7	0.9
6 2 0	21.9	19.6	8 4 4	17.6	19.5
5 3 3	0.8	0.6	7 5 5	2.1	0.6
6 2 2	1.3	1.8	7 7 1		0.6
4 4 4	7.4	7.0	9 3 3		0.6
5 5 1	1.3	0.5	8 6 0	0	0.5
7 1 1		0.5	10 0 0		0.1
6 4 0	0	0.3	8 6 2	58.9	42.6
6 4 2	27.3	24.3	10 2 0		21.3
5 5 3	1.9	0.4			
7 3 1		0.8			

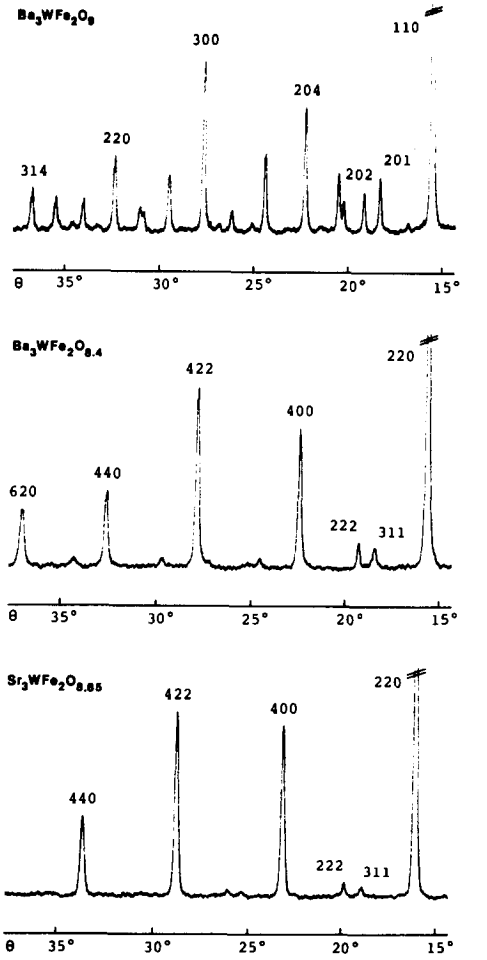

PHOTOGRAPH 3. X-Ray diffractograms of $Ba_3WFe_2O_9$ (hexagonal), $Ba_3WFe_2O_{8.4}$ (cubic), and $Sr_3WFe_2O_{8.85}$ (cubic).

(Photograph 3). But this comparison also points out the intensity differences between the corresponding lines and shows that $Ba_3WFe_2O_{8.4}$ is more similar to $Sr_3WFe_2O_{8.85}$ (cubic) than to $Ba_3WFe_2O_9$ (hexagonal) despite the replacement of Ba by Sr (Table V). The reflection number of the hexagonal structure is higher than that of the cubic structure. This difference does not appear in Table V because we only considered the lines which are common to both structures in order not to complicate this table, but it appears clearly in Photograph 3. In addition, the line intensities measured in the case of $Ba_3WFe_2O_9$ are often the sum of the intensities of two, three, or even four reflections which overlapped. This fact is due to the almost identical d values of the planes which are responsible for these reflections. To simplify Table V, we only gave for each common reflection the $(h\ k\ l)_h$ plane which contributes to the presence of this line and corresponds to a $(h'\ k'\ l')_c$ plane of the cubic lattice.

These $(h\ k\ l)$ planes of the hexagonal lattice which correspond to the $(h'\ k'\ l')$ planes of the cubic lattice were determined by the transformation matrix based on the precedent axis change formulas:

$$\begin{bmatrix} h \\ k \\ l \end{bmatrix}_{hex} = \begin{bmatrix} \frac{1}{2} & 0 & \frac{1}{2} \\ 0 & \frac{1}{2} & -\frac{1}{2} \\ -1 & 1 & 1 \end{bmatrix} \times \begin{bmatrix} h' \\ k' \\ l' \end{bmatrix}_{cub}$$

The values of the d distances (Table V) are lower for $Ba_3WFe_2O_{8.4}$ than for $Ba_3WFe_2O_9$. This difference emphasizes the cell contraction which is due to the structural change as it also appears on the X-ray photographs. The d values are even lower for $Sr_3WFe_2O_{8.85}$ (Table V and Photograph 3), the cell parameter of which is noticeably smaller than that of $Ba_3WFe_2O_{8.4}$ (7.888(2) Å instead of 8.105(2) Å), Sr^{2+} being smaller than Ba^{2+}.

Magnetic Measurements

The comparative magnetic study of $Ba_3WFe_2O_{8.4}$ with the starting hexagonal compound $Ba_3WFe_2O_9$ and the cubic strontium compounds $Sr_3WFe_2O_9$ and $Sr_3WFe_2O_{8.85}$ emphasizes the differences between the magnetic properties of both structures. Thus it confirms the existence of a cubic structure for $Ba_3WFe_2O_{8.4}$ as

TABLE V

I_{hkl} AND d_{hkl} VALUES FOR $Ba_3WFe_2O_9$ (*A*), $Ba_3WFe_2O_{8.4}$ (*B*), AND $Sr_3WFe_2O_{8.85}$ (*C*)

$h\ k\ l_A$	$h'\ k'\ l'_{B,C}$	I_A	I_B	I_C	d_A	d_B	d_C
1 0 1	1 1 1	2.6	4.9	2.1	4.711	4.679	4.554
1 0 2	2 0 0	2.0	1.1	2.3	4.080	4.053	3.944
1 1 0	2 2 0	100.0	100.0	100.0	2.886	2.866	2.789
2 0 1	3 1 1	8.9	5.0	2.3	2.460	2.444	2.378
2 0 2	2 2 2	7.2	6.0	2.6	2.356	2.340	2.277
2 0 4	4 0 0	21.9	36.7	38.4	2.040	2.026	1.972
2 1 1	3 3 1	13.5	2.2	1.0	1.872	1.859	1.810
2 1 2	4 2 0	1.2	0.9	1.4	1.825	1.812	1.764
3 0 0	4 2 2	28.6	52.3	45.6	1.666	1.654	1.610
3 0 3 3 0 3	3 3 3 5 1 1	8.8	2.8	0.8	1.570	1.560	1.518
2 2 0	4 4 0	12.6	24.8	21.0	1.442	1.433	1.394
3 1 1	5 3 1	4.7	2.5	0.8	1.379	1.370	1.333
3 1 2 3 0 6	4 4 2 6 0 0	0.6	0	0.3	1.360	1.351	1.315

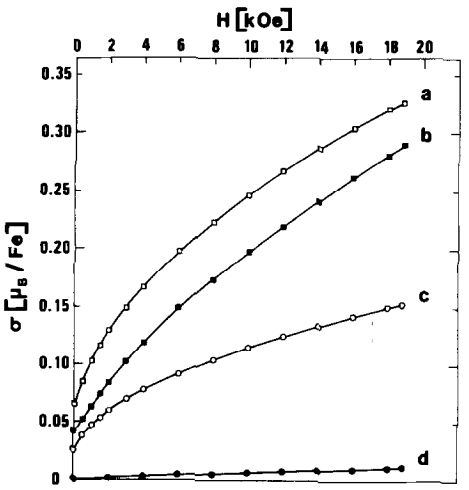

FIG. 1. Magnetization at 4.2 K versus magnetic field for (a) $Sr_3WFe_2O_{8.85}$, (b) $Ba_3WFe_2O_{8.4}$, (c) $Sr_3WFe_2O_9$, and (d) $Ba_3WFe_2O_9$.

shown by the comparative crystallographical study.

The measurements of magnetization at 4.2 K as a function of magnetic field (Fig. 1) as well as the study of magnetization (H = 18.8 kOe) versus temperature (Fig. 2) give curves which are analogous for the three cubic compounds, and characteristic of an unsaturated ferrimagnetism. The inverse susceptibility-vs-temperature plot above the Néel temperature for $Sr_3WFe_2O_9$ (*6*) confirms the existence of a Q ferrimagnetism. The magnetic behavior of the hexagonal compound is quite different: the variation of magnetization versus field is nearly linear (Fig. 1) and the value of the magnetization corresponding to the maximum field delivered by the magnetometer (H_{max} = 18.8 kOe) is noticeably lower than that of the cubic compounds.

The magnetization values obtained with this maximum field are similar for the cubic compounds and relatively high (between 0.15 and 0.30 μ_B/Fe) compared to that for $Ba_3WFe_2O_9$ ($\simeq$0.01 μ_B/Fe). Nevertheless they are much lower than the theoretical values of the saturated magnetizations, which can be easily calculated, taking into account the order rate between the cations distributed in the 4*a* and 4*b* sites. This nonsaturation of magnetization is often found in the W compounds, whereas the U compounds of the same family are easily

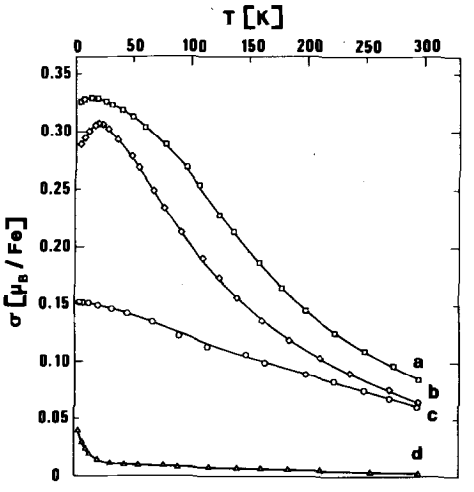

FIG. 2. Magnetization (H = 18.8 kOe) versus absolute temperature for (a) $Sr_3WFe_2O_{8.85}$, (b) $Ba_3WFe_2O_{8.4}$, and (c) $Sr_3WFe_2O_9$. Remanent magnetization as a function of absolute temperature for (d) $Ba_3WFe_2O_{8.4}$.

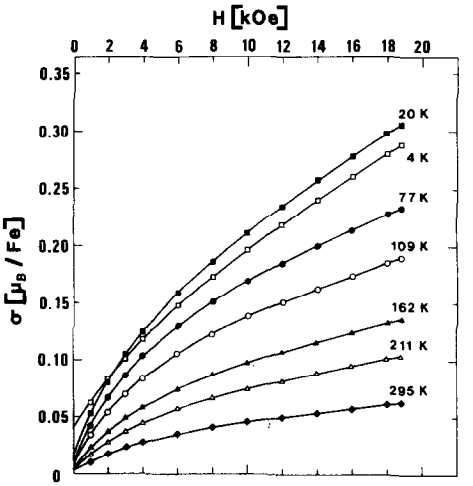

FIG. 3. Magnetization-vs-field plots of $Ba_3WFe_2O_{8.4}$ at low temperatures.

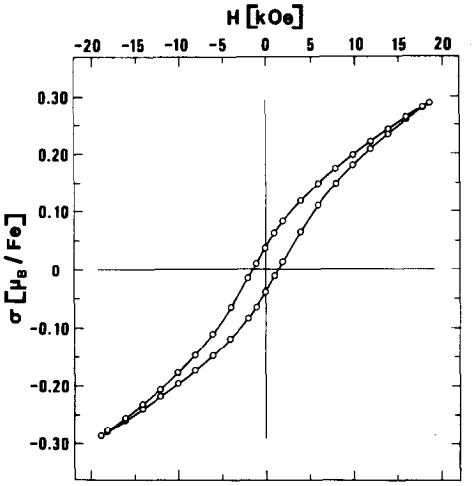

FIG. 4. The magnetization at 4.2 K of $Ba_3WFe_2O_{8.4}$ as a function of magnetic field.

saturated as is the case, for example, for the cubic ferrimagnetic compounds $Ba_3UFe_2O_9$ and $Sr_3UFe_2O_9$ (*11*). This phenomenon is particularly well illustrated by the study of Sévêque concerning the phase $Sr_3U_xW_{1-x}Fe_2O_9$ which shows a more and more easy saturation when the U percentage in the solid solution increases (*15*). It can also be noticed that $Ba_3WFe_2O_{8.4}$ has a slight remanent magnetization (Fig. 3) and consequently presents a hysteresis cycle (Fig. 4). The rapid decrease of this remanent magnetization with temperature (Fig. 2) as well as the relatively high value of the coercive field ($H_c \simeq 1300$ Oe at 4.2 K) shows that this remanent magnetization is not due to magnetite traces but is on the contrary an intrinsic property of the compound.

Therefore magnetic measurements allowed us, for the first time, to confirm the existence of a cubic structure for $Ba_3WFe_2O_{8.4}$. Mössbauer spectroscopic measurements should permit one to determine more precisely the kind and range of the magnetic interactions in this compound.

Conclusion

The principal purpose of the few studies which have been made up to now on the oxygen-deficient compounds has been to determine the vacancy distribution in the structure. Models have been proposed for $BaFeO_{3-x}$ (*3*) and $SrFeO_{3-x}$ (*10*), and for the system $CaTiO_3$–$Ca_2Fe_2O_5$ (*16*), based on neutron diffraction or electronic microscopy measurements.

For $Ba_3WFe_2O_{8.4}$, the average size increase of the cations in octahedral sites by reduction of the stoichiometric oxide seems to be more determining for the structure than the corresponding creation of oxygen vacancies, the percentage of which is relatively low, about 6%.

But our study of $Ba_3WFe_2O_{9-x}$ is, in fact, more than a new study of a structural change. Indeed it illustrates the importance of the choice of precise experimental conditions to get a well-defined compound and the variety of the products obtained from the same reagent mixture according to the heat treatment used. Finally, this study principally emphasizes the importance of a slight nonstoichiometry resulting from the experimental conditions for the structure and the properties of a phase.

References

1. F. SÉVÊQUE, P. DELAMOYE, P. POIX, AND A. MICHEL, *C. R. Acad. Sci. Paris Ser. C* **269**, 1536 (1969).
2. J. BERTHON, Thèse de doctorat d'Etat, Orsay (1976).
3. A. J. JACOBSON, *Acta Crystallogr. Sect. B* **32**, 1087 (1976).
4. G. MATZEN, F. SÉVÊQUE, AND P. POIX, *Z. Anorg. Allg. Chem.*, in press.
5. P. POIX, *Sem. Chim. Etat Solide* **I**, 82 (1966–1967).
6. D. BALLUTAUD-HARARI, Thèse de doctorat d'Etat, Orsay (1975).
7. L. KATZ AND R. WARD, *Inorg. Chem.* **3**, 205 (1964).
8. "International Tables for X-Ray Crystallography," Vol. 1, p. 304, Kynoch Press, Birmingham (1952).

9. "International Tables for X-Ray Crystallography," Vol. 1, p. 338, Kynoch Press, Birmingham (1952).
10. B. C. TOFIELD, C. GREAVES, AND B. E. F. FENDER, *Mater. Res. Bull.* **10,** 737 (1975).
11. C. ROPARS, J. BERTHON, J. C. BERNIER, AND P. POIX, *Ann. Chim. (Paris)* **1,** 377 (1966).
12. D. T. CROMER AND J. T. WABER, *Acta Crystallogr.* **18,** 104 (1965).
13. D. T. CROMER, *Acta Crystallogr.* **18,** 17 (1965).
14. M. TOKONAMI, *Acta Crystallogr.* **19,** 486 (1965).
15. F. SÉVÊQUE, Thèse de 3ème cycle, Orsay (1970).
16. J. C. GRENIER, G. SCHIFFMACHER, P. CARO, M. POUCHARD, AND P. HAGENMULLER, *J. Solid State Chem.* **20,** 365 (1977).